Journal Homepage: http://ijcpe.uobaghdad.edu.iq
Iraqi Journal of Chemical and Petroleum Engineering
Vol. 27 No. 1 (March 2026) 155 – 167
EISSN: 2618-0707, PISSN: 1997-4884

# Adopting the addition of iron waste as a source for iron (II) ion in Electro-Fenton system for the removal of triple dyes

**Huda N. Jaber** [a], **Rasha H. Salman** [a, *]

*a Department of Chemical Engineering, College of Engineering, University of Baghdad, Baghdad, Iraq*

## Abstract

Use of electrodes that provide a high surface area for reaction, such as Nickel foam and Carbon Fiber Felt, has proven highly efficient in treating wastewater. In this study, a mixture of dyes (Eosin Y, Methylene Blue, and Methylene Violet) was treated using Ni foam as a cathode and carbon fiber felt as an anode in the Electro-Fenton process, relying on iron waste, such as iron filings, as the catalyst source. The analysis characterization of electrodes and iron filings was determined by Energy dispersive X-Ray (EDX) and Scanning electron microscopy (SEM) tests. The results showed high efficiency in decomposing the dye mixture. The highest Re % 96.4591 which attained after accomplishing the experiments based on Response Surface Method (RSM) was recorded at 75 mA of current, 0.25 g/L of iron filings concentration, and 0.015 M of electrolyte concentration. The highest specific energy expenditure for this process was 6.892939 kWh/kg of dyes. In addition to the process's energy efficiency, using iron scrap as a cheap alternative to expensive iron salts is a cost-effective and environmentally friendly approach.

*Keywords: Triple Dyes; Electro-Fenton; Iron Filings; Response Surface Methodology; Ni-Foam; Carbon Fiber Felt.*

*Received on 09/02/2026, Received in Revised Form on 14/03/2026, Accepted on 14/03/2026, Published on 30/03/2026*

*https://doi.org/10.31699/IJCPE.2026.1.13*

## 1- Introduction

One of the most significant environmental challenges facing the world today is the presence of organic pollutants, especially industrial dyes and complex organic compounds, due to their chemical stability, difficulty in biodegradation, and toxic effects on ecosystems and living organisms.

Among the most widely used and common dyes in the textile and cosmetic industries are Eosin Y, methyl blue (MB), and methyl violet (MV). Although the concentrations of these dyes in natural waters vary and are not precisely measured, these dyes pose an environmental risk that significantly affects the health of water bodies and living organisms [1- 3].

Traditional methods of water treatment, such as physical or biological treatment [4, 5], have proven limited in their effectiveness in removing pollutants of this type, and this has prompted researchers to develop advanced and highly efficient technologies [6].

Advanced oxidation processes (AOPs) are one of these technologies that have emerged as a promising solution for treating stubborn organic pollutants [7]. The generation of hydroxyl radicals ($OH^{\bullet}$), which are characterized by their high ability to break down and oxidize organic compounds and dyes into less toxic products such as $CO_2$ and $H_2O$, is the basis on which this process depends [8-10]. The Electro-Fenton (EF) process combines the electrochemical reaction and the traditional Fenton reaction through the electrical generation of iron (II) ($Fe^{2+}$) ions and hydrogen peroxide ($H_2O_2$) as shown in Eqs. 1 to 3, so it is considered one of the most efficient advanced oxidation techniques [11, 12].

$$Fe + 2H^{+} \rightarrow Fe^{2+} + H_2 \quad (1)$$

$$O_2 + 2H^{+} + 2e^{-} \rightarrow H_2O_2 \quad (2)$$

$$H_2O_2 + Fe^{2+} \rightarrow OH^{\bullet} + OH^{-} + Fe^{3+} \quad (3)$$

Accurate control of operating conditions, low consumption of chemical reagents, high efficiency of hydroxyl radicals' generation, and high ability to treat organic pollutants even with low concentrations are among the most important features of the EF process [13]. Therefore, this process has received increasing attention in the field of industrial and environmental wastewater treatment and has become one of the important topics in research studies [14, 15].

The EFP reaction begins within the electrochemical cell when an electric current is applied between the electrodes. $H_2O_2$ is formed by the reduction of dissolved oxygen at the cathode Eq. 2. Hydrogen peroxide generation is a crucial step in the process because this compound is the primary reactant in the Fenton reaction. Simultaneously, $Fe^{2+}$ are supplied to the medium, either by direct addition to the solution as iron salts or by electrochemical generation from an iron anode within the cell or by releasing iron ion (II) from iron waste Eq. 1 [16, 17].

---

*Corresponding Author: Email: rasha.habeeb@coeng.uobaghdad.edu.iq

After the formation of $H_2O_2$ and the presence of $Fe^{2+}$, the Fenton reaction occurs. Ferrous ions react with hydrogen peroxide to produce OH radicals and $Fe^{3+}$ Eq. 3 [18, 19]. When OH radicals react with dyes pollutants (R) Eq. 4, $OH^{\bullet}$ break the chemical bonds within molecules, particularly aromatic bonds or double bonds found in many toxic organic compounds and dyes, leading to the formation of simpler intermediate compounds. These intermediate compounds are subjected to repeated attacks by $OH^{\bullet}$ as the reaction continues, leading to their gradual decomposition into smaller molecules such as short-chain organic acids, and ultimately into stable inorganic products such as $CO_2$, $H_2O$, and inorganic ions Eqs. 5 and 6 [20]. A key advantage of the EF process is that the $Fe^{3+}$ produced by the Fenton reaction can be reduced again at the cathode to $Fe^{2+}$, thus continuing the iron cycle within the system without the need for the continuous addition of large quantities of iron [21].

$$OH\bullet + R \rightarrow R\bullet + H_2O \tag{4}$$

$$R\bullet + O_2 \rightarrow ROO\bullet \tag{5}$$

$$OH\bullet + intermediate \rightarrow CO_2 + H_2O + inorganic\ ions \tag{6}$$

The efficiency of the EF process is mainly affected by the type of electrodes used, as it controls the nature of electrochemical reactions, the rate of generation of active oxidizing species, and system stability during operation as well [22]. The efficiency of generating $H_2O_2$ and regenerating $Fe^{2+}$ necessary for the continuation of the Fenton reaction at the cathode is affected by the type of electrode material, Physical structure, surface area, and the electrical conductivity nature of the electrode. Supporting oxidation reactions and reducing the accumulation of intermediate products within the reaction medium is one of the anode electrode roles [7, 23].

Enhancing mass transfer and increasing the number of active sites for electrochemical reactions, which reflects positively on the performance of the EF process, is achieved by using materials with a high surface area and porous structure for the cathode electrode, such as Cu foam [24] Ni foam activated carbon fiber (ACF) [25], and others. In contrast, the anode requires high electrochemical stability to avoid corrosion and dissolution, in addition to a high ability to contribute to the oxidation of pollutants or the by-products while maintaining the stability of the reactive medium [23]. Due to the three-dimensional structure of nickel foam, effective surface area, and high porosity, which in turn improves electrochemical reactions and charge transfer within the EF system, this research relied on using the Ni foam electrode as a cathode.

Due to the electrochemical stability of the carbon fiber felt (CFF) electrode and its resistance to corrosion, in addition to its support for oxidation reactions within the system without the release of metal ions that may affect the stability of the reactive medium or the treatment products [22], this electrode was used as an anode in this study. To reduce operational costs and manage waste disposal to preserve the ecosystem, it was decided to use iron waste (IW), such as iron filings (IF), as a heterogeneous source of catalyst ($Fe^{2+}$) [23, 26].

This study aims to stabilize the effectiveness of the EF system using a Ni foam as a cathode and a CFF as anode and the effect of current and electrolyte concentration for treating water from a mixture of dyes (Eosin Y, methylene blue (MB), and methylene violet (MV)) using IF as a source of the catalyst.

## 2- Experimental work

### 2.1. Materials

Ni foam and Carbon Fiber Felt (CFF) were imported from China, and Iron Filings (If) from local iron workshop. The chemical materials used in this work were: sodium sulfate ($Na_2SO_4$) (Sisco Research Laboratories Pvt. Ltd., Ind.), sulfuric acid ($H_2SO_4$) (SDFCL, Ind.), and sodium hydroxide (NaOH) (Alpha Chemika, Ind.). Table 1 illustrates the chemical structure and properties of dyes used, and the calibration curve of mixture of three dyes, which shows that the dyes mixing didn't cause any interloping of the dyes which cause no problem in measuring the concentration of any dyes.

### 2.2. Experimental methods

An individual 1-liter glass batch reactor was used for all experiments, filling with 0.75 L of simulated wastewater containing 75 mg/L of mixture of dyes (Eosin Y, MB, and MV), 25 mg/L for each dye. Fig. 1 shows the schematic diagram of the EF system.

The solution was mixed at 300 rpm using a magnetic stirrer (Stu art CD-162, Biocote) at 30°C and aerated for 20 minutes before the reaction began by pumped air into reaction solution using pump (HAILEA, model ACO-208, China), and the airflow rate was controlled at 20 L/h using an air flowmeter.

The dimensions used for the nickel-foam plate (cathode) and the carbon fiber-felt (anode) were 140 mmm × 60 mm × 9 mm, and 140 mm × 60 mm × 2 mm, respectively. A 10 mm thick Perspex cover with several holes was used on the glass reactor to maintain a 30 mm spacing between the electrodes during the reaction and for sample collection. A 650 × 110 × 2 mm Perspex frame was used to fix the CFF electrode due to its flexible fabric structure. The Ni foam electrode surface, before any run, was cleaned from any pollutants with 0.1 M of H2SO4 solution then washed with distillated water and dried at 80 °C for several hours.

$Na_2SO_4$ was added to improve the electrical conductivity of the solution [27]. And to supply the solution with the necessary $Fe^{2+}$ (Fenton reagent), concentrations for the Fenton reaction [28], Iron Filings, which washed with distilled water and dried for 24 hours at 85°C, were added.

Since the ideal pH for the Fenton reaction is between 2.5 and 3.5 [29], a 0.1 M sulfuric acid and sodium hydroxide solutions were used to neutralize and stabilize the pH at 3.

To provide the required current between the electrodes, a power supply (MAISHENG MS-605D) was used to maintain the current at the desired level for 30 minutes.

Samples were collected during the reaction using a pipette, and the sample concentration was measured using a UV-9200 spectrometer. The concentration at the specified time was then applied to Eq. 7 to calculate the removal efficiency [30].

$$Re\% = \frac{Co-Cf}{Co} \times 100 \tag{7}$$

Where Re % is the removal efficiency, $C_o$ is the initial concentration of the solution (mg/L), and $C_f$ is the final concentration of the collected sample (mg/L).

Eq. 8 was used to calculate the specific energy consumption [31].

$$SEC = \frac{I \times V \times 1000}{\Delta m} \tag{8}$$

Where SEC is specific energy consumption (kWh/kg of dyes), I is the applied current (mA), V is the voltage (volt.), and Δm is the difference in weight of the dyes during reaction (kg).

A tintometer GmbH RD125 (SN 0214/5767, Dortmund Lovibond co., Germany) was used to measure the COD content in the samples before and after the reaction.

**Table 1.** Dyes properties and chemical structure

| Dyes | Chemical Formula | Chemical Structure | Wavelength (nm) | Calibration Curve |
|---|---|---|---|---|
| Eosin Y | $C_{20}H_6Br_4Na_2O_5$ | 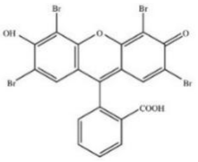 | 517 | 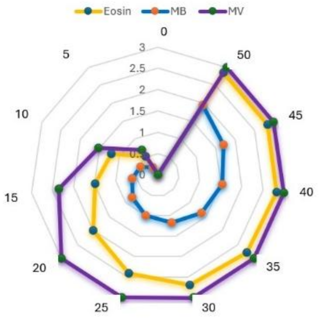 |
| MB | $C_{16}H_{18}ClN_3S$ | 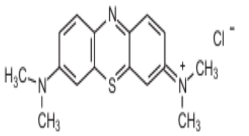 | 690 | |
| MV | $C_{14}H_{12}N_2OS$ | 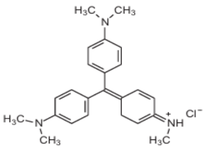 | 580 | |

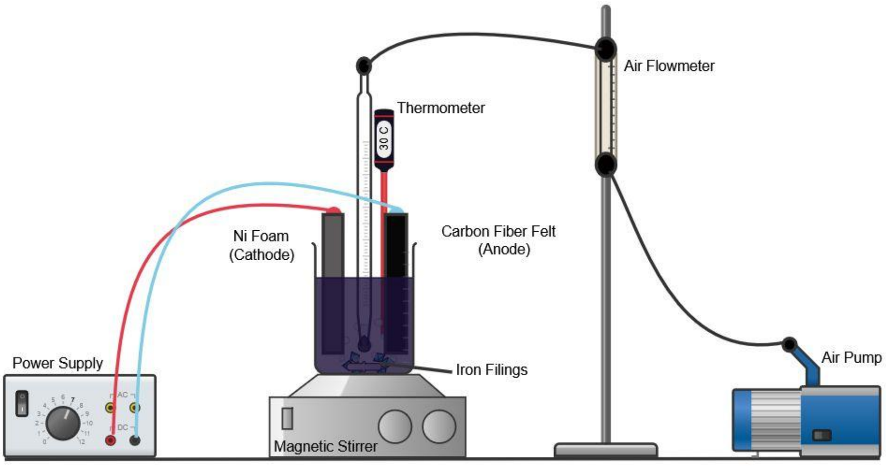

**Fig. 1.** The schematic diagram of the EF system

## 2.3. Design of experimental

The analysis and modeling of the studied response is performed using software Minitab-22 comprised of a set of statistical and mathematical methods known as Response Surface Methodology (RSM) [32]. This methodology examines the optimal conditions for achieving the desired response by studying a set of variables that influence response [33]. To optimize and study the effect of operating variables on the removal of a dye mixture in this study, using nickel foam as the cathode and carbon fiber felt as the anode in Electro-Fenton system, a Box-Benken design (BBD) was employed. This design yields three levels, grouped across 15 experiments [34]. The factors are I (X1), Fe filings (X2), and $Na_2SO_4$ (X3) and the response is Re % as shown in Table 2, where -1, 0, and +1 represent the minimum, middle, and maximum values for each input variables, respectively. Table 3 also presents the process design, represented by the actual and coded values.

**Table 2.** Process variables and their levels for dyes mixture removal efficiency

| Variables | Units | Sample | Low (-1) | Middle (0) | High (+1) |
|---|---|---|---|---|---|
| Current | mA | X1 | 25 | 50 | 75 |
| Iron filings | g/L | X2 | 0.25 | 0.875 | 1.5 |
| $Na_2SO_4$ | M | X3 | 0.01 | 0.015 | 0.02 |

**Table 3.** BBD design for dyes mixture removal efficiency

| Run | Coded value | | | Actual value | | |
|---|---|---|---|---|---|---|
| | X1 | X2 | X3 | Current (mA) | Iron filings (g/L) | $Na_2SO_4$ (M) |
| 1 | +1 | 0 | -1 | 75 | 0.875 | 0.010 |
| 2 | -1 | -1 | 0 | 25 | 0.250 | 0.015 |
| 3 | +1 | -1 | 0 | 75 | 0.250 | 0.015 |
| 4 | -1 | 0 | +1 | 25 | 0.875 | 0.020 |
| 5 | 0 | -1 | -1 | 50 | 0.250 | 0.010 |
| 6 | -1 | 0 | -1 | 25 | 0.875 | 0.010 |
| 7 | 0 | -1 | +1 | 50 | 0.250 | 0.020 |
| 8 | +1 | +1 | 0 | 75 | 1.500 | 0.015 |
| 9 | 0 | 0 | 0 | 50 | 0.875 | 0.015 |
| 10 | -1 | +1 | 0 | 25 | 1.500 | 0.015 |
| 11 | +1 | 0 | +1 | 75 | 0.875 | 0.020 |
| 12 | 0 | 0 | 0 | 50 | 0.875 | 0.015 |
| 13 | 0 | +1 | -1 | 50 | 1.500 | 0.010 |
| 14 | 0 | +1 | +1 | 50 | 1.500 | 0.020 |
| 15 | 0 | 0 | 0 | 50 | 0.875 | 0.015 |

## 2.4. Electrode characterization

The cathode (Ni foam) and anode (CFF) surface were examined by using Scanning Electron Microscope (SEM). Fig. 2 (b) illustrates the 3D network structure of Ni foam with distribution of different multiple interconnected pores. And Fig. 3 (b) shows the interwoven capillary structure of CFF, with tiny gaps appearing between the capillary structures of the electrode. And the purity of the electrodes material is examined by utilizing Energy Dispersive X-ray Spectroscopy (EDX) as shown in Fig. 2 (a) and Fig. 3 (a).

## 2.5. Iron filings characterization

Fig. 4 (a and b) shows the EDX and SEM of Iron Filings, and illustrates the random shapes of IF, which are a result of the iron cutting process and have not yet undergone any specific shaping process. Just wash with distilled water to remove any dirt or impurities and dried at 80 °C for several hours. Therefore, Fig. 4 (b) also shows the IF composed of 62.64 % of iron and 37.36 % of oxygen. This is what was determined by washing with distilled water. And the absence of any other elements in the analysis of the components makes it a pure source of the catalyst ($Fe^{2+}$) used in this study.

| Element | Weight % |
|---|---|
| Ni | 100.00 |
| Total | 100.00 |

**Fig. 2.** a) EDX and b) SEM of Ni Foam before used as cathode in EF process

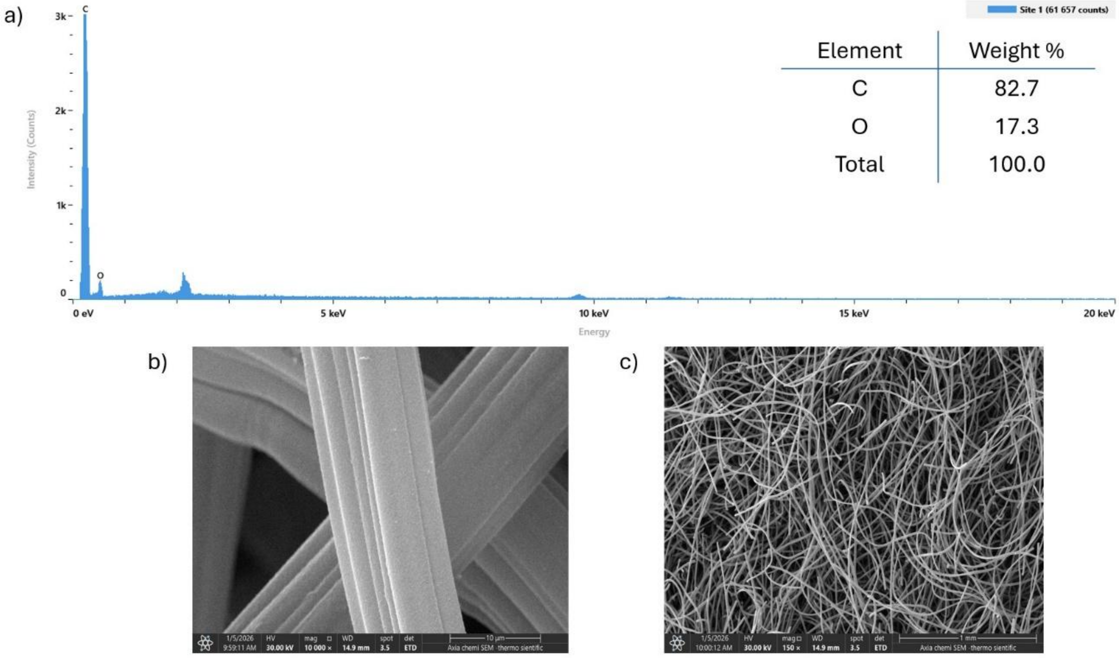

| Element | Weight % |
|---|---|
| C | 82.7 |
| O | 17.3 |
| Total | 100.0 |

**Fig. 3.** a) EDX, b) refers 10 µm, and c) refers 1 µm SEM of CFF before used as anode in EF process

| Element | Weight % |
|---|---|
| O | 37.36 |
| Fe | 62.64 |
| Total | 100.00 |

**Fig. 4.** a) EDX and b) SEM of Iron Filings

## 3- Results and discussion

### 3.1. Analytic of static

The quadratic Eq. 9, attained by using Minitab-22 software, was used to clarify the relation between the removal efficiency and the studied parameters, and estimate the predicted Re %. The actual Re % and predicted Re % are illustrated in Table 4.

$$Re\,\% = 73.74 - 0.227 \times I + 6.99 \times [Fe] + 2807 \times [Na_2SO_4] + 0.00455 \times I \times I - 5.55 \times [Fe] \times [Fe] - 93048 \times [Na_2SO_4] \times [Na_2SO_4] - 0.0166 \times I \times [Fe] - 6.33 \times I \times [Na_2SO_4] - 213 \times [Fe] \times [Na_2SO_4] \quad (9)$$

As illustrated in Table 4 the Re % range, as shown in run (14) and run (3), was between 76.53 to 96.6814 %. As shown in run (4) and run (1) the specific energy consumption range was between 0.739321 to 6.892939 kWh/kg of dyes, and these values are considered to represent low to medium energy consumption [25].

The Re % increased from 88.6755 to 95.2994 % by increasing the current from 25 to 75 mA, with fixing the concentration of $Na_2SO_4$ and Fe filings at 0.01 M and 0.875 g/L respectively, as shown in run (6) and run (1). That clarifies the proportional effect of current factor on removal efficiency. Which can relate that to when the current increases the electron transfer through electrodes increases which leads to more production of OH• and in turn increases the degradation of the dye's molecules [35].

By comparing run (7) and run (14) when Fe filings concentration increases from 0.25 to 1.5 g/L and with fixing the current at 50 mA and $Na_2SO_4$ at 0.02 M the Re % decreases from 87.6658 to 76.53 %. This explains the inverse relationship between the removal efficiency and Fe filings. These can be attributed to the fact that $Fe^{2+}$ are gradually released from the iron filings at a concentration of 0.25 g/L in proportion to the amount of hydrogen peroxide generated during the reaction, thus allowing the Fenton reaction to proceed [16, 17].

However, when a concentration higher than 0.25 g/L is used, the released Fe ions become so numerous that they consume the generated hydroxyl radicals and produce $Fe^{3+}$, which hinders the completion of the Fenton reaction and results in a decrease in the removal efficiency of dyes mixture [22, 36].

By comparing two runs (1) and (11), when the current and iron filings concentration were fixed at 75 mA and

0.875 g/L respectively, and the sodium sulfate concentration was increased from 0.01 to 0.02 M, the removal efficiency decreased from 95.2994 to 87. 8707 %, i.e. with a difference of 7.4287%. This decrease is less to 2.5674 % when the same range of sodium sulfate is used and the current is fixed at 50 mA and the iron filings at 0.25 g/L, i.e. run (5) and run (7). This can be attributed to the fact that increasing the $Na_2SO_4$ concentration leads to an increase in the system's conductivity, i.e., an increase in $H_2O_2$ production and consequently an increase in hydroxyl radical generation. Due to the gradual release of $Fe^{2+}$, the amount of hydrogen peroxide accumulates in the system, causing a decrease in hydroxyl radical generation and thus delaying the completion of the oxidation process of the dyes, and as a result, the removal efficiency decreases [37, 38].

## 3.2. ANOVA analysis

The significance and suitability of polynomial quadratic model that was recommended by BBD was evaluated by studied analysis of variance (ANOVA). The ANOVA specify by used degree of freedom (DF), contribution, sum of squares (SS), mean of squares (MS), adjust sum of squares (Adj. SS), Adjust mean of squares (Adj. MS), F-value, and P-value.

The linear term contribution was 75.67%, while the square term and 2=way interaction term contribution were 20.91 and 1.32 % respectively. The model is significant, as demonstrated by low P-value (0.001) and high F-value (25.89). F-value represented by the ratio of mean square model (MS) to the mean square error. While the P-value represents the probability value that evaluates the effect of statistically significant. The low P-value (less than 0.05) and high F-value (more than 4) represent the statically significant of variables [39, 40]. 97.90 % of $R^2$ indicates the good fitting of model with experimental data. The ANOVA analysis, Table 5 illustrates that the factors studied affect the Re% in the following order: iron filings ($X_2$) have the greatest impact on removal efficiency, followed by current ($X_1$), then $Na_2SO_4$ ($X_3$), with P-value 0.000, 0.001, and 0.002, and F-value 98.40, 48.90, and 32.76, respectively.

**Table 4.** The obtained actual and predicted removal efficiency of dyes mixture and the specific energy consumption of the process

| Run | Current (mA) | Iron filings (g/L) | $Na_2SO_4$ (M) | Actual Re% | Predicted Re% | Voltage | Specific Energy Consumption (kWh/kg of dyes) |
|---|---|---|---|---|---|---|---|
| 1 | 75 | 0.875 | 0.010 | 95.2994 | 95.2687 | 13.0 | 6.892939 |
| 2 | 25 | 0.250 | 0.015 | 89.0724 | 90.2068 | 5.4 | 1.021887 |
| 3 | 75 | 0.250 | 0.015 | 96.4591 | 96.6814 | 9.3 | 4.871196 |
| 4 | 25 | 0.875 | 0.020 | 84.4099 | 84.4406 | 3.7 | 0.739321 |
| 5 | 50 | 0.250 | 0.010 | 90.2332 | 90.0416 | 7.5 | 2.801648 |
| 6 | 25 | 0.875 | 0.010 | 88.6755 | 87.7327 | 5.0 | 0.950475 |
| 7 | 50 | 0.250 | 0.020 | 87.6658 | 86.5007 | 5.8 | 2.230792 |
| 8 | 75 | 1.500 | 0.015 | 88.8492 | 87.7148 | 9.9 | 5.634656 |
| 9 | 50 | 0.875 | 0.015 | 88.6020 | 88.5434 | 6.0 | 2.283053 |
| 10 | 25 | 1.500 | 0.015 | 82.5031 | 82.2808 | 3.7 | 0.756617 |
| 11 | 75 | 0.875 | 0.020 | 87.8707 | 88.8135 | 8.2 | 4.719658 |
| 12 | 50 | 0.875 | 0.015 | 88.5604 | 88.5434 | 7.7 | 2.93131 |
| 13 | 50 | 1.500 | 0.010 | 81.7630 | 82.9281 | 8.1 | 3.343115 |
| 14 | 50 | 1.500 | 0.020 | 76.5300 | 76.7216 | 5.3 | 2.339026 |
| 15 | 50 | 0.875 | 0.015 | 88.4677 | 88.5434 | 8.0 | 3.048744 |

**Table 5.** ANOVA analysis

| Source | DF | Seq SS | Contribution | Adj SS | Adj MS | F-Value | P-Value |
|---|---|---|---|---|---|---|---|
| Model | 9 | 337.798 | 97.90 % | 337.798 | 37.533 | 25.89 | 0.001 |
| Linear | 3 | 261.094 | 75.67 % | 261.094 | 87.031 | 60.02 | 0.000 |
| I (mA) | 1 | 70.909 | 20.55 % | 70.909 | 70.909 | 48.90 | 0.001 |
| Fe filings (g/L) | 1 | 142.680 | 41.35 % | 142.680 | 142.680 | 98.40 | 0.000 |
| $Na_2SO_4$ (M) | 1 | 47.505 | 13.77 % | 47.505 | 47.505 | 32.76 | 0.002 |
| Square | 3 | 72.156 | 20.91 % | 72.156 | 24.052 | 16.59 | 0.005 |
| I (mA)*I (mA) | 1 | 37.464 | 10.86 % | 29.922 | 29.922 | 20.64 | 0.006 |
| Fe filings (g/L)* Fe filings (g/L) | 1 | 14.712 | 4.26 % | 17.373 | 17.373 | 11.98 | 0.018 |
| $Na_2SO_4$ (M)*$Na_2SO_4$ (M) | 1 | 19.980 | 5.79 % | 19.980 | 19.980 | 13.78 | 0.014 |
| 2-Way Interaction | 3 | 4.548 | 1.32 % | 4.548 | 1.516 | 1.05 | 0.449 |
| I (mA)* Fe filings (g/L) | 1 | 0.271 | 0.08 % | 0.271 | 0.271 | 0.19 | 0.684 |
| I (mA)* $Na_2SO_4$ (M) | 1 | 2.501 | 0.72 % | 2.501 | 2.501 | 1.73 | 0.246 |
| Fe filings (g/L)*$Na_2SO_4$ (M) | 1 | 1.776 | 0.51 % | 1.776 | 1.776 | 1.23 | 0.319 |
| Error | 5 | 7.250 | 2.10 % | 7.250 | 1.450 | - | - |
| Lack-of-Fit | 3 | 7.240 | 2.10 % | 7.240 | 2.413 | 511.14 | 0.002 |
| Pure Error | 2 | 0.009 | 0.00 % | 0.009 | 0.005 | - | - |
| Total | 14 | 345.048 | 100.00 % | - | - | - | - |
| Model summery | | | S | $R^2$ % | $R^2$ (adj.) % | Press | $R^2$ (Pred.)% |
| | | | 1.20415 | 97.90 | 94.12 | 115.868 | 66.42 |

### 3.3. The effect of the factors studied

From Fig. 5 (a, and b) it is evident that increasing the current leads to an increase in Re%. This is caused by an increase in the generation of $H_2O_2$, by increase reduction of $O_2$ on the cathode surface, and consequently an increase in the production of hydroxyl radicals, and as a result an increase in the oxidation process of the pollutant (dyes mixture), which enhance the degradation of dyes [41, 42].

Fig. 6 (a, and b) shows that increasing the concentration of IF in the process is undesirable because the Fenton reaction fundamentally depends on the availability of the catalyst, i.e., Fe (II), and generation of hydroxyl radicals. Since iron filings are a heterogeneous source of $Fe^{2+}$, meaning that the release of $Fe^{2+}$ occurs gradually during the reaction time, the low IF concentration releases enough ions for the Fenton reaction. However, increasing the amount of IF leads to an increase in the release of ions for the catalyst. Consequently, the available $Fe^{2+}$ concentration competes with the production of OH•, which $Fe^{2+}$ react with $H_2O_2$ to produce ferric ions. This resulted in a decrease in the amount of hydroxyl radicals needed for the Fenton reaction. Furthermore, this step inhibits the continuation of the EF reaction [16, 17, 37].

As can be seen from Fig. 7 (a, and b), the best Re% occurs at a $Na_2SO_4$ concentration below 0.015 M. This is because the electrolyte improves the system's conductivity, leading to increased oxygen reduction at the cathode surface, i.e. Ni Foam, and consequently, increased $H_2O_2$ generation. Since the IF releases $Fe^{2+}$ gradually, disproportionate to the amount of generated hydrogen peroxide, this causes an increase in concentration and accumulation of $H_2O_2$ in the solution. This, in turn, slows down the $Fe^{3+}/Fe^{2+}$ cycle and leads to hydroxyl radical generation [42, 43].

### 3.4. Test of optimization and confirmation

The optimal conditions of factors used in this study were predicted by using the Minitab-22 software with BBD analysis methods. Table 6 shows the predictions of this analysis, and Table 7 illustrates the results obtained by applying the predicted values, which were within the expected response of the Minitab-22 program, which in turn proves that the program is analytical and statistical and can be relied upon in analyzing the results of experiments. COD testing was also performed, before and after experiment, under these optimal conditions, and these values were 17 and 0 mg/L, respectively, indicating a 100% COD removal. The comparison with the previous study as illustrated in Table 8 emphasized that the present study has an excellent results.

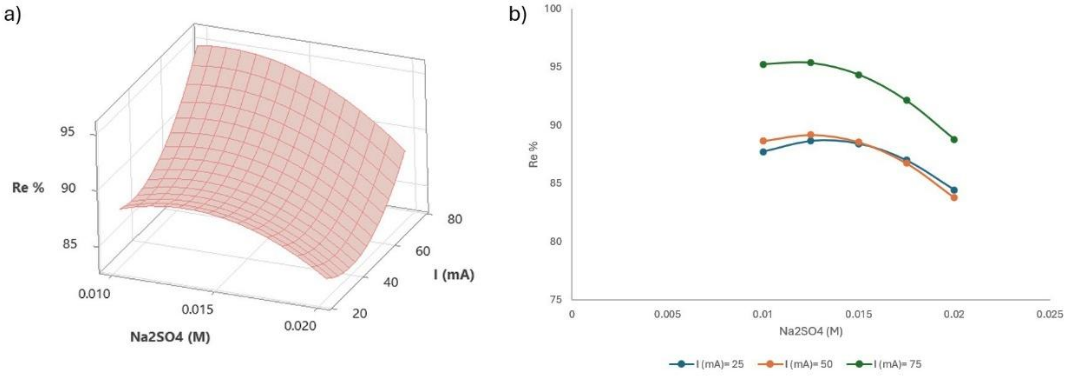

**Fig. 5.** (a) 3D plot (b) 2D plot for dyes mixture Re % at IF = 0.875 g/L, and different concentrations of $Na_2SO_4$ and I

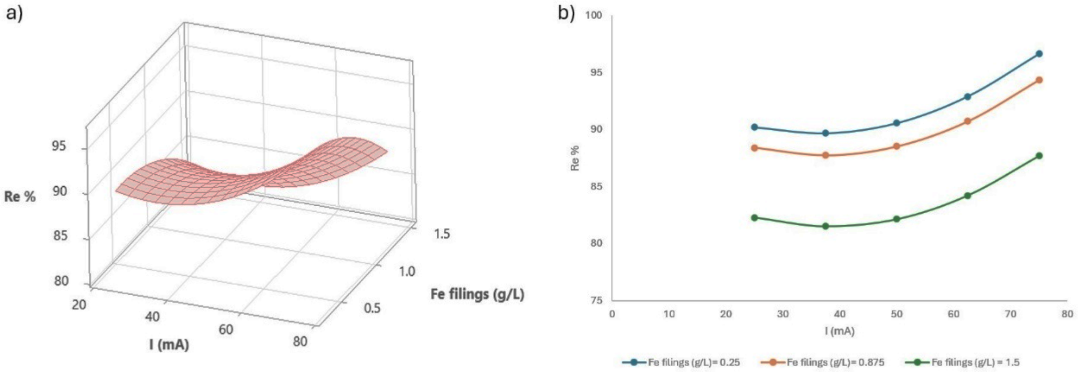

**Fig. 6.** (a) 3D plot (b) 2D plot for dyes mixture Re % at $Na_2SO_4$ = 0.015 M, and different concentrations of IF and I

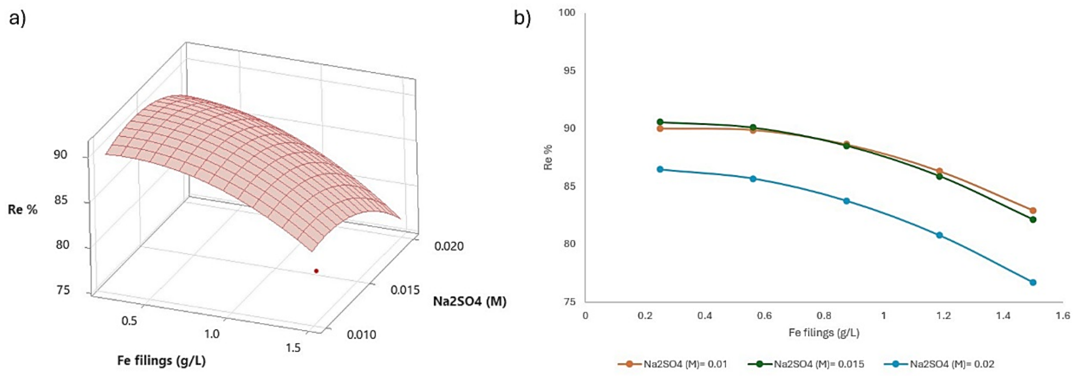

**Fig. 7.** (a) 3D plot (b) 2D plot for dyes mixture Re % at I = 50 mA, and different concentrations of IF and $Na_2SO_4$

**Table 6.** Variables performance of optimal system for maximum dyes mixture removal

| Response | Goal | Lower | Target | Upper | Weight | Importance |
|---|---|---|---|---|---|---|
| Dyes mixture Re% | Maximum | 76.53 % | 96.6814 % | | 1 | 1 |
| **Solution of parameter** | | | **Prediction of multiple response** | | | |
| I (mA) | Iron filings (g/L) | $Na_2SO_4$ (M) | Re % fit. | 95 % CI | 95 % PI | Desirability of Composite |
| 75 | 0.2878 | 0.0122 | 97.39 | 95.60 | 93.23 | 1 |

**Table 7.** Dyes removal experiment confirmation

| Run | I (mA) | Iron filings (g/L) | $Na_2SO_4$ (M) | V (volt.) | SEC (KW/Kg) | Re % | Average |
|---|---|---|---|---|---|---|---|
| 1 | 75 | 0.2878 | 0.0122 | 7.5 | 4.044871103 | 93.71 | 94.335 % |
| 2 | 75 | 0.2878 | 0.0122 | 7.7 | 4.097488293 | 94.96 | |

**Table 8.** Comparison the results of current study with some of previous studies

| Dye | Electrodes | Process conditions | Re % | References |
|---|---|---|---|---|
| MB | Anode:<br>Iron<br>Cathode:<br>Iron | $Na_2SO_4$: 0.05 M<br>Current: 78 mA<br>Catalyst source: electrolysis of iron electrode.<br>Time: 8.5 min. | 99.8 | [44] |
| MB | Anode:<br>Pt<br>Cathode:<br>Graphite | $Na_2SO_4$: 0.05 M<br>Current: 150 mA<br>Catalyst source: Sep/$FeS_2$<br>Time: 75 min. | 96.6 | [45] |
| MB | Anode:<br>Stainless steel meshes<br>Cathode:<br>Stainless steel meshes | $Na_2SO_4$: 0.5 M<br>Current: 100 mA<br>Catalyst source: Iron Salt (FeSO4.7H2O)<br>Time: 80 min. | 99 | [46] |
| MV | Anode:<br>Titanium<br>Cathode:<br>Graphite | $Na_2SO_4$: 0.2 M<br>Current: 2 A<br>Catalyst source: Iron-biochar (pistachio shells)<br>Time: 60 min. | 98.8 | [47] |
| MO | Anode:<br>Porous Graphite<br>Cathode:<br>Copper Foam | $Na_2SO_4$: 0.02 M<br>Current: 339.3 mA<br>Catalyst source: Iron Waste.<br>Time: 35 min. | 98.82 | [17] |
| Eosin + MB+ MV | Anode:<br>Carbon Feber Felt<br>Cathode:<br>Ni Foam | $Na_2SO_4$: 0.015 M<br>Current: 75 mA<br>Catalyst source: Iron Filings.<br>Time: 30 min. | 96.4591 | Recent work |

### 3.5. Electrode characterization

Fig. 8 (a) shows that after using Ni foam as a cathode, some components of the reaction solution, such as Fe, C, and Na, are deposited on its surface, along with a slight change in the surface resulting from the passage of current and the reduction of $O_2$ on the nickel foam surface as shown in Fig. 8 (b).

Fig. 9 (a, and b) shows the EDX and SEM of CFF, which clarify the deposition of the reaction solution components on the CFF capillaries structure during the reaction, with slight scattering of the electrode structure resulting after its use as an electrode for the process.

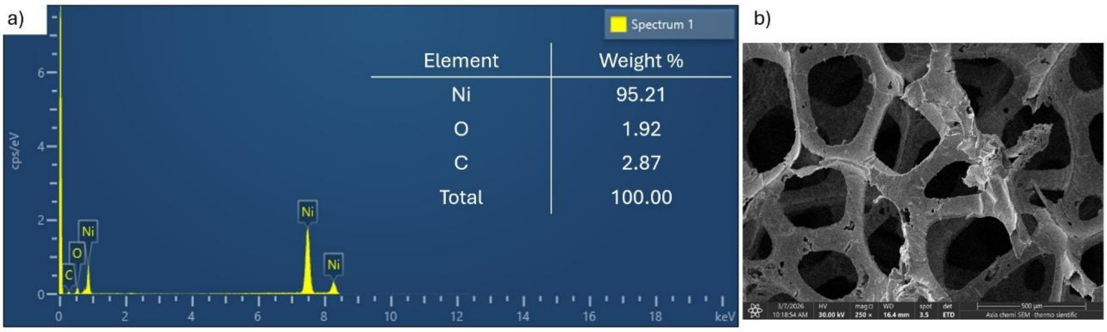

| Element | Weight % |
|---|---|
| Ni | 95.21 |
| O | 1.92 |
| C | 2.87 |
| Total | 100.00 |

**Fig. 8.** a) EDX and b) SEM of Ni Foam after using as cathode in EF system

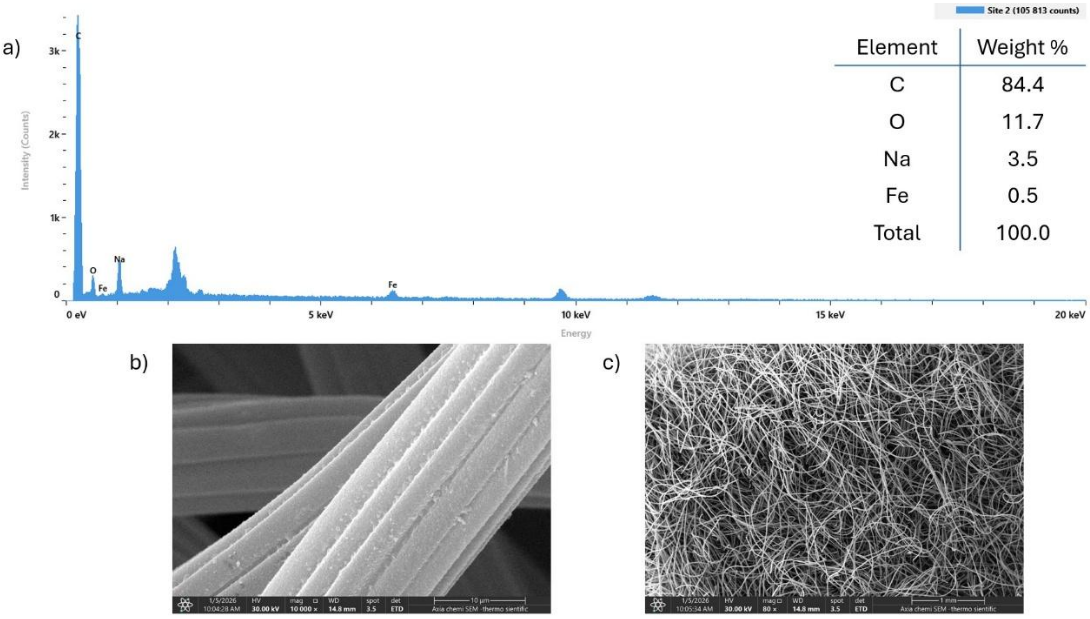

| Element | Weight % |
|---|---|
| C | 84.4 |
| O | 11.7 |
| Na | 3.5 |
| Fe | 0.5 |
| Total | 100.0 |

**Fig. 9.** a) EDX, b) refers 10 µm, and c) refers µm SEM of CFF after using as anode in EF system

## 4- Conclusion

This work investigated the effect of several factors, i.e. current, IF, and $Na_2SO_4$ concentrations, on the removal of a dye mixture using the EF technique with Ni foam as the cathode and CFF as the anode, relying on IF as the source of $Fe^{2+}$ as a catalyst for this process. RSM using a Box-Benken design was employed to Optimize and analyze the data for the studied variables. The results showed that IF had the greatest effect on the removal efficiency, as increasing the concentration of IF consequently reduced the Re% of dye mixture due to the gradual release of $Fe^{2+}$. The effect of current was the second most important factor in the removal efficiency, showing a direct correlation between current and Re%. Increasing the current leads to fast degradation of dyes, thus improving the removal efficiency. The highest removal rate was achieved at the highest current used in this study, i.e., 75 mA. The best Re% was achieved at $Na_2SO_4$ concentration below 0.015 M, as increasing the electrolyte concentration leads to an enhancement of $H_2O_2$ production and accumulation of $H_2O_2$ at low concentration of IF, resulting in decreased of Re%. Furthermore, using IF as available and inexpensive alternative to costly iron salts reduces the cost of the process and makes it easier to implement and more environmentally friendly.

## Nomenclature

| | |
|---|---|
| EF | Electro-Fenton |
| RSM | Response Surface Methodology |
| BBD | Box-Behnken Design |
| CFF | Carbon Fiber Felt |
| Re % | Removal Efficiency of Dyes Mixture |
| $C_0$ | Initial Concentration of Dyes Mixture (mg/L) |
| $C_f$ | Final Concentration of Dyes Mixture (mg/L) |
| SEC | Specific Energy Consumption (kWh/kg) |
| I | Current (mA) |
| V | Voltage (v) |
| $\Delta C$ | Different in Dyes Mixture Concentration (mg/L) |
| IF | Irin Filings |
| X1 | Current Coded Value (mA) |
| X2 | Iron Filings Coded Value (g/L) |
| X3 | $Na_2SO_4$ Concentration Coded Value (M) |

## References

[1] R. Manivannan, J. Ryu, and Y. A. Son, “Photo discoloration of eosin yellow dye under visible light using TiO2@TPPS nanocomposite synthesized via ultrasonic assisted method,” *Colloids and Surfaces A: Physicochemical and Engineering Aspects*, 2021. https://doi.org/10.1016/j.colsurfa.2020.125601

[2] A. Tkaczyk-wliz, K. Mitrowska, and B. Tomasz, “Quantification of twenty pharmacologically active dyes in water samples using UPLC-MS / MS,” *Heliyon*, vol. 8, no. April, 2022. https://doi.org/10.1016/j.heliyon.2022.e09331

[3] M. I. Al-zaban, N. K. Alharbi, F. M. Albarakaty, S. Alharthi, S. H. A. Hassan, and M. A. Fawzy, “Experimental modeling investigations on the biosorption of methyl Violet 2B dye by the Brown seaweed cystoseira tamariscifolia,” *Sustainability*, vol. 14, 2022. https://doi.org/10.3390/su14095285

[4] H. Sukmana, N. Bellahsen, F. Pantoja, and C. Hodur, “Adsorption and coagulation in wastewater treatment - Review,” *Progress in Agricultural Engineering Sciences*, vol. 17, no. 1, 2021, pp. 49–68. https://doi.org/10.1556/446.2021.00029

[5] M. Hube, Selina Eskafi, B. Hrafnkelsdóttir, Kolbrún Fríða Bjarnadóttir, M. Á. Bjarnadóttir, and B. Axelsdóttir, Snærós Wu, “Direct membrane filtration for wastewater treatment and resource recovery: A review,” *Science of the Total Environment*, 2020. https://doi.org/10.1016/j.scitotenv.2019.136375

[6] J. J. Pignatello, E. Oliveros, and A. Mackay, “Advanced oxidation processes for organic contaminant destruction based on the Fenton reaction and related chemistry,” *Environmental Science and Technology*, vol. 36, no. 1, 2007, pp. 1–84. https://doi.org/10.1080/10643380500326564

[7] I. Sirés, E. Brillas, M. A. Oturan, M. A. Rodrigo, and M. Panizza, “Electrochemical advanced oxidation processes : today and tomorrow . A review,” *Springer*, vol. 21, 2014, pp. 8336–8367. https://doi.org/10.1007/s11356-014-2783-1

[8] M. A. Oturan and J. Aaron, “Advanced oxidation processes in water / wastewater treatment : principles and applications . A review,” *Environmental Science and Technology*, vol. 44, no. 23, 2014, pp. 2577–2641. https://doi.org/10.1080/10643389.2013.829765

[9] I. H. Dakhil and A. S. Abbas, “Challenges and future directions in photoelectro-Fenton techniques : A comprehensive review of emerging applications and innovations,” *Iraqi Journal of Chemical and Petroleum Engineering*, vol. 26, no. 3, 2025, pp. 63–83. https://doi.org/10.31699/IJCPE.2025.3.7

[10] P. K. Pandis *et al.*, “Key points of advanced oxidation processes ( AOPs ) for wastewater , organic pollutants and pharmaceutical waste treatment : A mini review,” *Chemengineering*, vol. 6, no. 8, 2022. https://doi.org/10.3390/chemengineering6010008

[11] V. Kaswan and H. Kaur, “A comparative study of advanced oxidation processes for wastewater treatment,” *Water Practice & Technology*, vol. 18, no. 5, 2023, pp. 1233–1254. https://doi.org/10.2166/wpt.2023.061

[12] E. Brillas, I. Sire, and M. A. Oturan, “Electro-Fenton Process and Related Electrochemical Technologies Based on Fenton ’ s Reaction Chemistry,” *Chemical Reviews*, vol. 109, 2009, pp. 6570–6631. https://doi.org/10.1021/cr900136g

[13] A. Alterkaoui, H. Arslan, M. Saleh, N. Dizge, D. Balakrishnan, and N. Naik, “Integrated electro-Fenton and membrane filtration technologies for effective organic pollutant removal and salt recovery from Sesame process wastewater,” *Springer*, 2025. https://doi.org/10.1186/s40068-025-00410-w

[14] I. Sirés and E. Brillas, “Remediation of water pollution caused by pharmaceutical residues based on electrochemical separation and degradation technologies : A review,” *Environment International*, vol. 40, 2012, pp. 212–229. https://doi.org/10.1016/j.envint.2011.07.012

[15] S. O. Ganiyu, C. A. Martínez-huitle, and M. A. Oturan, “ScienceDirect Electrochemistry Electrochemical advanced oxidation processes for wastewater treatment : Advances in formation and detection of reactive species and mechanisms,” *Current Opinion in Electrochemistry*, vol. 27, no. December 2020, 2021, p. 100678. https://doi.org/10.1016/j.coelec.2020.100678

[16] Z. Heidari, R. Pelalak, R. Alizadeh, N. Oturan, and S. Shirazian, “Application of mineral iron-based natural catalysts in Electro-Fenton process: A comparative study,” *Catalyst*, vol. 11, no. 57, 2021, pp. 1–18. https://doi.org/10.3390/catal11010057

[17] Z. M. Hameed & R. H. Salman, “Optimizing methyl orange degradation via electro-Fenton with copper foam cathode: A comparative approach using iron waste vs. iron salts and exploring catalyst and cathode Durability,” *Applied Science and Engineering Process*, vol. 18, no. 4, 2025, p. 7728. https://doi.org/10.14416/j.asep.2025.05.002

[18] M. Umar, H. A. Aziz, and M. S. Yusoff, “Trends in the use of Fenton, electro-Fenton and photo-Fenton for the treatment of landfill leachate,” *Waste Management*, vol. 30, no. 11, 2010, pp. 2113–2121. https://doi.org/10.1016/j.wasman.2010.07.003

[19] M. J. Nuhma, O. A. Mohsen, Kh. M. Abed, K. F. Zageer, Bilal A. Wasim, and A. A. Hassan, “Electro-Fenton oxidation for degradation of direct Red organic pollutants using stainless steel and iron electrodes,” in *The Eurasia Proceedings of Science, Technology, Engineering & Mathematics (EPSTEM)*, 2025, pp. 1124–1134. https://doi.org/10.55549/epstem.1376

[20] H. Liu, C. Wang, X. Li, X. Xuan, C. Jiang, and H. N. Cui, "A novel electro-Fenton process for water treatment: Reaction-controlled pH adjustment and performance assessment," *Environmental Science and Technology*, vol. 41, no. 8, 2007, pp. 2937–2942. https://doi.org/10.1021/es0622195

[21] D. Li, T. Zheng, Y. Liu, D. Hou, K. K. Yao, W. Zhang, H. Song, H. He, W. Shi, L. Wang, and J.Ma, "A novel Electro-Fenton process characterized by aeration from inside a graphite felt electrode with enhanced electrogeneration of H2O2 and cycle of Fe3+/Fe2+," *Journal of Hazardous Materials*, vol. 396, no. January, 2020, p. 122591. https://doi.org/10.1016/j.jhazmat.2020.122591

[22] L. Chen, Song, Tang, G. Feng, Haopeng, Zhou, Yaoyu, Zeng, J. Lu, Yue, Yu, B. Ren, Xiaoya, Peng, and X. Liu, "Carbon felt cathodes for electro-Fenton process to remove tetracycline via synergistic adsorption and degradation," *Science of the Total Environment*, vol. 670, 2019, pp. 921–931. https://doi.org/10.1016/j.scitotenv.2019.03.086

[23] H. Ding, Q. Ma, X. Zhang, C. Wang, N. You, and S. Deng, "Material design and operation strategy of the Electro-Fenton system for the treatment of high pollutant load wastewater," *Sustainability*, 2025, pp. 1–25. https://doi.org/10.3390/su172310501

[24] Zahraa M. Hameed and R. H. Salman, "Elimination of methyl Orange dye with three dimensional Electro-Fenton and Sono-Electro-Fenton systems utilizing copper foam and activated carbon," *Ecological Engineering & Environmental Technology*, vol. 25, no. 10, 2024, pp. 44–59. https://doi.org/10.12912/27197050/191199

[25] B. Ramírez-pereda, A. Alvarez-gallegos, J. G. Rangel-peraza, and Y. A. Bustos-terrones, "Kinetics of Acid Orange 7 oxidation by using carbon fi ber and reticulated vitreous carbon in an electro-Fenton process," *Journal of Environmental Management*, vol. 213, 2018. https://doi.org/10.1016/j.jenvman.2018.01.022

[26] P. Natarajan, J. S. Gulliver, and W. A. Arnold, "Iron filings application to reduce lake sediment phosphorus release," *Lake and Reservoir Management*, vol. 37, no. 2, 2021, pp. 143–159. https://doi.org/10.1080/10402381.2020.1862371

[27] D. Ghernaout and B. Ghernaout, "On the controversial effect of sodium sulphate as supporting electrolyte on electrocoagulation process : A review," *Desalination and Water Treatment*, vol. 27, no. 1–3, 2011, pp. 243–254. https://doi.org/10.5004/dwt.2011.1983

[28] M.S. Bala, A.A. Mohd Azoddein, M.I. Ahdash, and B.Y. Alshwal, "Comparative study for activation of hydrogen peroxide by chemical reagents (Fe2+, Al3+) to reduce chemical oxygen demand in petrochemical wastewater," *Journal of Engineering and Technology*, vol. 9, no. 2, 2018.

[29] L. Chachou, Y. Gueraini, Y. Bouhalouane, S. Poncin, H.Z. Li, and K. Bensadoka, "Application of electro-Fenton process for cutting fluids mineralization," *Environmental Technology*, no. February, 2015, pp. 37–41. https://doi.org/10.1080/09593330.2015.1016120

[30] F. C. Moreira, R. A. R. Boaventura, E. Brillas, and V. J. P. Vilar, "Environmental Electrochemical advanced oxidation processes : A review on their application to synthetic and real wastewaters," *"Applied Catalysis B: Environmental,"* vol. 202, 2017, pp. 217–261. https://doi.org/10.1016/j.apcatb.2016.08.037

[31] L. Zhou, J. Li, F. Li, Q. Meng, J. Li, and X. Xu, "Energy consumption model and energy efficiency of machine tools : a comprehensive literature review," *Journal of Cleaner Production*, 2016. https://doi.org/10.1016/j.jclepro.2015.05.093

[32] S. Ben, K. Davide, C. Sourour, C. Elaoud, and M. Panizza, "Response surface methodology for low - energy consumption electro - Fenton process for xanthene dye electrochemical degradation," *Journal of Applied Electrochemistry*, vol. 54, no. 9, 2024, pp. 2095–2110. https://doi.org/10.1007/s10800-024-02087-y

[33] A. Ahmadi, S. Heidarzadeh, A. R. Mokhtari, E. Darezereshki, and H. A. Harouni, "Optimization of heavy metal removal from aqueous solutions by maghemite (γ-Fe2O3) nanoparticles using response surface methodology," *Journal of Geochemical Exploration*, 2014. https://doi.org/10.1016/j.gexplo.2014.10.005

[34] K. P. Singh, A. K. Singh, and U. V. Singh, "Optimizing removal of ibuprofen from water by magnetic nanocomposite using Box – Behnken design," *Environmental Science and Pollution Research*, 2012, pp. 724–738. https://doi.org/10.1007/s11356-011-0611-4

[35] Z. I. Abbas and A. S. Abbas, "Optimization of the electro-Fenton process for COD reduction from refinery wastewater," *Environmental Engineering and Management Journal*, vol. 19, no. 11, 2020, pp. 2029–2037. https://doi.org/10.30638/eemj.2020.192

[36] G. K. S. Mortazavian, A. S. N. Zamani, and M. H. Hasheminejad, "Treatment of composting leachate using electro - Fenton process with scrap iron plates as electrodes," *International Journal of Environmental Science and Technology*, 2019. https://doi.org/10.1007/s13762-018-2057-4

[37] X. Wang, J. Zhao, C. Song, X. Shi, and H. Du, "An Eco-friendly iron cathode Electro-Fenton system coupled with a pH-regulation electrolysis cell for p-nitrophenol degradation," *Frontiers in Chemistry*, vol. 9, no. January, 2022, pp. 1–10. https://doi.org/10.3389/fchem.2021.837761

[38] M. Rostamizadeh, A. Jafarizad, and S. Gharibian, “High efficient decolorization of Reactive Red 120 azo dye over reusable Fe- ZSM-5 nanocatalyst in Electro-Fenton reaction,” *Separation and Purification Technology*, 2018. https://doi.org/10.1016/j.seppur.2017.10.041

[39] R. N. Henson, *Analysis of Variance (ANOVA)*, vol. 1. Elsevier Inc., 2015. https://doi.org/10.1016/B978-0-12-397025-1.00319-5

[40] A. F. Al-alawy and M. K. Al-ameri, “Treatment of simulated oily wastewater by ultrafiltration and nanofiltration processes,” *Iraqi Journal of Chemical and Petroleum Engineering*, vol. 18, no. 1, 2017, pp. 71–85. https://doi.org/10.31699/IJCPE.2017.1.6

[41] H. H. Thwaini and R. H. Salman, “Modification of Electro-Fenton Process with Granular Activated Carbon for Phenol Degradation – Optimization by Response Surface Methodology,” *Journal of Ecological Engineering*, vol. 24, no. 9, 2023, pp. 92–104. https://doi.org/10.12911/22998993/168411

[42] Y. Zheng, S. Qiu, F. Deng, Y. Zhu, G. Li, and F. Ma, “Three-dimensional electro-Fenton system with iron foam as particle electrode for folic acid wastewater pretreatment,” *Separation and Purification Technology*, vol. 224, no. February, 2019, pp. 463–474. https://doi.org/10.1016/j.seppur.2019.05.054

[43] A. A. Majed, A. H. Abbar, and E. Kamberli, “Efficient treatment of petroleum refinery wastewater by an induced electro-Fenton process,” *Iraqi Journal of Chemical and Petroleum Engineering*, vol. 26, no. 4, 2025, pp. 53–62. https://doi.org/10.31699/IJCPE.2025.4.5

[44] S. Zahedi, A. Asadipour, M. Dolatabadi, and S. Ahmadzadeh, “Response surface modeling for the treatment of methylene blue from aqueous media using electro-Fenton process before determination by UV-Vis spectrometer : Kinetic and degradation mechanism,” *Analytical Methods in Environmental Chemistry Journal*, vol. 5, no. 2, 2022, pp. 39–50. https://doi.org/10.24200/amecj.v5.i02.178

[45] M. F. M. G. Motlagh, “Electrochemical mineralization of methylene blue dye using electro - Fenton oxidation catalyzed by a novel sepiolite / pyrite nanocomposite,” *International Journal of Environmental Science and Technology*, vol. 2, no. 1, 2020. https://doi.org/10.1007/s13762-020-02749-2

[46] M. Loloei and A. Rezaee, “Decolorization of methylene blue by the electro - Fenton process using stainless steel mesh electrodes,” *International Journal of Environmental Health Engineering*, 2016, pp. 1–6.

[47] S. Madhi *et al.*, “Transforming waste to purity : 3D electro-Fenton process boosted with pistachio shell-derived iron-biochar electrode for methyl violet 2B dye catalytic removal,” *Desalination and Water Treatment*, vol. 320, no. August, 2024, p. 100845. https://doi.org/10.1016/j.dwt.2024.100845

# اعتماد إضافة نفايات الحديد كمصدر لأيون الحديد (II) في نظام إلكترو– فنتون لإزالة أصباغ ثلاثية

**هدى نعمة جابر [١]، رشا حبيب سلمان [١، *]**

*١ قسم الهندسة الكيمياوية، كلية الهندسة، جامعة بغداد، بغداد، العراق*

## الخلاصة

أثبت استخدام الأقطاب الكهربائية ذات المساحة السطحية العالية للتفاعل، مثل رغوة النيكل ولباد ألياف الكربون، كفاءة عالية في معالجة مياه الصرف الصحي. في هذه الدراسة، عُولج خليط من الأصباغ (إيوسين Y، أزرق الميثيلين، وبنفسجي الميثيلين) باستخدام رغوة النيكل ككاثود ولباد ألياف الكربون كأنود في عملية إلكترو–فنتون، بالاعتماد على نفايات الحديد، مثل برادة الحديد، كمصدر للمحفز. حُددت خصائص الأقطاب الكهربائية وبرادة الحديد باستخدام مطيافية تشتت طاقة الأشعة السينية (EDX) والمجهر الإلكتروني الماسح (SEM). أظهرت النتائج كفاءة عالية في تحليل خليط الأصباغ. سُجلت أعلى نسبة كفاءة (Re%) بلغت ٩٦.٤٥٩١، والتي تحققت بعد إجراء التجارب بناءً على منهجية سطح الاستجابة (RSM)، عند تيار ٧٥ مللي أمبير، وتركيز برادة حديد ٠.٢٥ غ/لتر، وتركيز إلكتروليت ٠.٠١٥ مولاري. بلغ أعلى معدل استهلاك للطاقة النوعية لهذه العملية ٦.٨٩٢٩٣٩ كيلوواط.ساعة/كيلوغرام من الأصباغ. إضافةً إلى كفاءة الطاقة في هذه العملية، يُعدّ استخدام خردة الحديد كبديل رخيص لأملاح الحديد باهظة الثمن نهجًا فعالًا من حيث التكلفة وصديقًا للبيئة.

**الكلمات الدالة:** صبغات ثلاثية، الكتروفنتون، منهجية سطح الاستجابة، رغوة النيكل، لباد الياف الكربون.